Robust Trajectory Tracking for a Reversing Tractor Trailer

Cédric Pradalier and Kane Usher
Autonomous Systems Laboratory
CSIRO ICT Centre
P.O. Box 883
Kenmore, QLD 4069, Australia
e-mail: cedric.pradalier@mavt.ethz.ch, k.usher@uq.edu.au

Received 11 November 2007; accepted 15 March 2008

Tractor-trailer reversing is a classical nonlinear control problem in which many of the solutions proposed in the literature perform poorly in the presence of real-world constraints such as steering angle, rate limits, and lags. In this paper we describe a new method in which an inner loop controls the hitch angle of the trailer, creating a virtual articulated vehicle to which existing control techniques can be applied. We provide an analysis of the stability and convergence properties of this control approach, as well as experimental results that illustrate the robustness of this approach to model estimation errors, low-level control loop dynamics, and other disturbances introduced by, for example, state estimation errors. © 2008 Wiley Periodicals, Inc.

1. INTRODUCTION

Reversing of tractor-trailer systems is a common task in both recreational and industrial settings. In the recreational domain, examples of tractor-trailer reversing tasks include parking of transportation trailers and the reversing of boat trailers onto boat ramps. A driver-aid or automation system for performing such tasks could be of significant benefit for inexperienced or unskilled drivers.

In industrial settings, examples of tractor-trailer systems include agricultural systems, transportation, and cargo handling. Generally, drivers in industry are well trained and experience little difficulty in achieving a desired tractor-trailer reversing trajectory. However, a growing number of these tasks are being automated, for which a robust and reliable control system is essential.

Most existing approaches address the problem through the development of complex, nonlinear controllers, which can prove to be difficult to implement and tune. Furthermore, few, if any, of these approaches can deal with slow steering loop dynamics and limits, and many of these methods also fail in the face of significant noise in the system state estimation.

By reformulating the problem such that the input to the system is the angle between the tractor and trailer (i.e., the hitch angle) rather than the tractor steering angle, the system can be treated as a "virtual" articulated vehicle. Closing the inner loop on the hitch angle can be achieved using a proportional–integral (PI) controller, and the outer loop on the trajectory can be closed with very simple methods based on path lateral, longitudinal, and orientation errors. This paper extends earlier work (Pradalier & Usher,

2007a, 2007b) by providing a more thorough theoretical analysis of the properties of this control approach.

The remainder of this paper is structured as follows: Section 2 defines the problem addressed, including the kinematic model of the tractor-trailer system; Section 3 reviews existing approaches and discusses the problems with these approaches as applied to platforms with significant underlying control loop dynamics; Section 4 outlines our approach to trajectory control and discusses in depth the hitch-angle stabilization loop; Section 5 describes the platform and the properties of the system considered in this paper, Section 6 outlines comprehensive experiments validating the approach, and Section 7 concludes the paper.

2. PROBLEM MOTIVATION

The problem addressed in this work is that of reversing a tractor-trailer system onto a preplanned trajectory in the face of very slow steering loop dynamics and steering angle range limitations. The system should also be tolerant to noise in the available pose estimates. Additionally, as the system is targeted as a driver aid or as an automation system for industrial robots, it should rely on minimal computational and sensory resources, be easy to implement and tune, and be tolerant to plant variation.

The geometry of the tractor-trailer system considered here is depicted in Figure 1. The lengths referred to in this figure are defined as follows: L, the distance between the front and rear axles of the tractor; L_1, the distance between the rear axle of the trailer and the hitch joint; and L_2, the distance between the trailer axle and the hitch joint.

The system states are described by (x, y), the Cartesian coordinate of point P in the global frame; θ_1 and θ_2, the heading of the tractor and trailer, respectively; and ψ, the hitch angle (note that $\theta_2 = \theta_1 + \psi$). The system is controlled via two inputs: v, the linear velocity of point P ($v = \|\dot{P}\|$); and ϕ, the steering angle of the front wheels. With this notation, the system can be described by the following equations:

$$\dot{x} = v\cos\theta_1, \tag{1}$$

$$\dot{y} = v\sin\theta_1, \tag{2}$$

$$\dot{\theta}_1 = \frac{v\tan\phi}{L}, \tag{3}$$

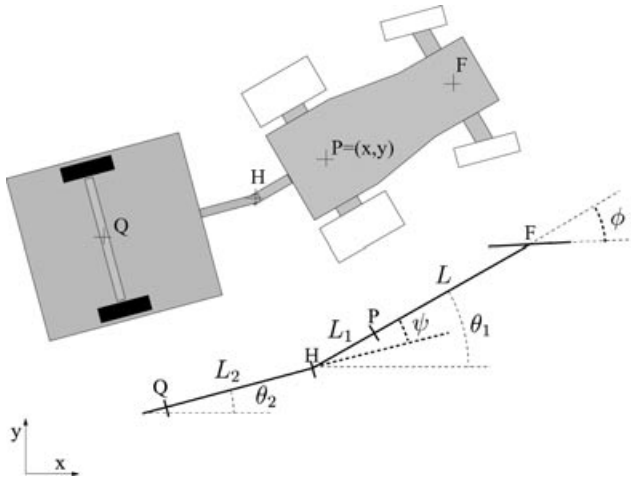

Figure 1. Kinematic model of a tractor-trailer system. It is particularly important to note the definition of the steering angle ϕ and the hitch angle ψ, i.e., the angle between the tractor and the trailer.

$$\dot{\psi} = \frac{-v\tan\phi}{L}\left(\frac{L_1}{L_2}\cos\psi + 1\right) - \frac{v}{L_2}\sin\psi. \tag{4}$$

The first three equations of this system are the standard kinematics for a car-like vehicle; see, e.g., De Luca and Oriolo (1995) for a derivation. Proving the expression for $\dot{\psi}$ requires consideration of the speed V_H of point H (resp. P or Q) in the global frame. First, we define $\Omega_1 = [0, 0, \dot{\theta}_1]^T$ and $\Omega_2 = [0, 0, \dot{\theta}_2]^T$. Then,

$$V_H = V_P + \Omega_1 \times \boldsymbol{PH}, \tag{5}$$

$$V_H = V_Q + \Omega_2 \times \boldsymbol{QH}. \tag{6}$$

with $\theta_2 = \theta_1 + \psi$ and where bold italic notation represents vectors. The expression for $\dot{\psi}$ is derived by solving

$$V_P + \Omega_1 \times \boldsymbol{PH} = V_Q + \Omega_2 \times \boldsymbol{QH}. \tag{7}$$

3. REVIEW OF EXISTING APPROACHES

The control of tractor-trailer systems has received much attention in the scientific and patent literature (see, e.g., Carter & Lormor, 2004; Karl, 1987; Robert, 2004) as it has clear industrial applications and is also interesting due to its inherent nonlinear

nature. In this section, we review several approaches to the problem and present representative examples of our testing of these approaches. To do this, we use the kinematic model of the tractor-trailer system [Eqs. (1)–(4)] and introduce additional dynamics in the steering response through rate limiting.

3.1. Stabilization Using a Virtual Tractor

The first method tested in this review relies on the idea that there exists a unique one-to-one mapping between the speed vector of a point on the tractor and the speed vector of a point on the trailer (Sekhavat, Lamiraux, Laumond, Bauzil, & Ferrand, 1997) (see Figure 1). Knowing this relation, it is possible to "virtually" exchange the role of the tractor and trailer. Given the distance from the trailer to the reference trajectory, a simple controller, such as pure pursuit (Hebert, Thorpe, & Stentz, 1997), can give the desired translational and rotational speed for the trailer. This control vector can then be mapped to a control vector for the tractor.

Experimentally, this method is able to stabilize the system, provided that we assume there are no limits on the steering angle rate. When even modest steering rate limits are introduced, the performance quickly degrades. Figure 2 illustrates this degradation: at a steering rate limit of 110 deg/s, control is still effective if not oscillatory, and at 100 deg/s, stabilization is no longer possible.

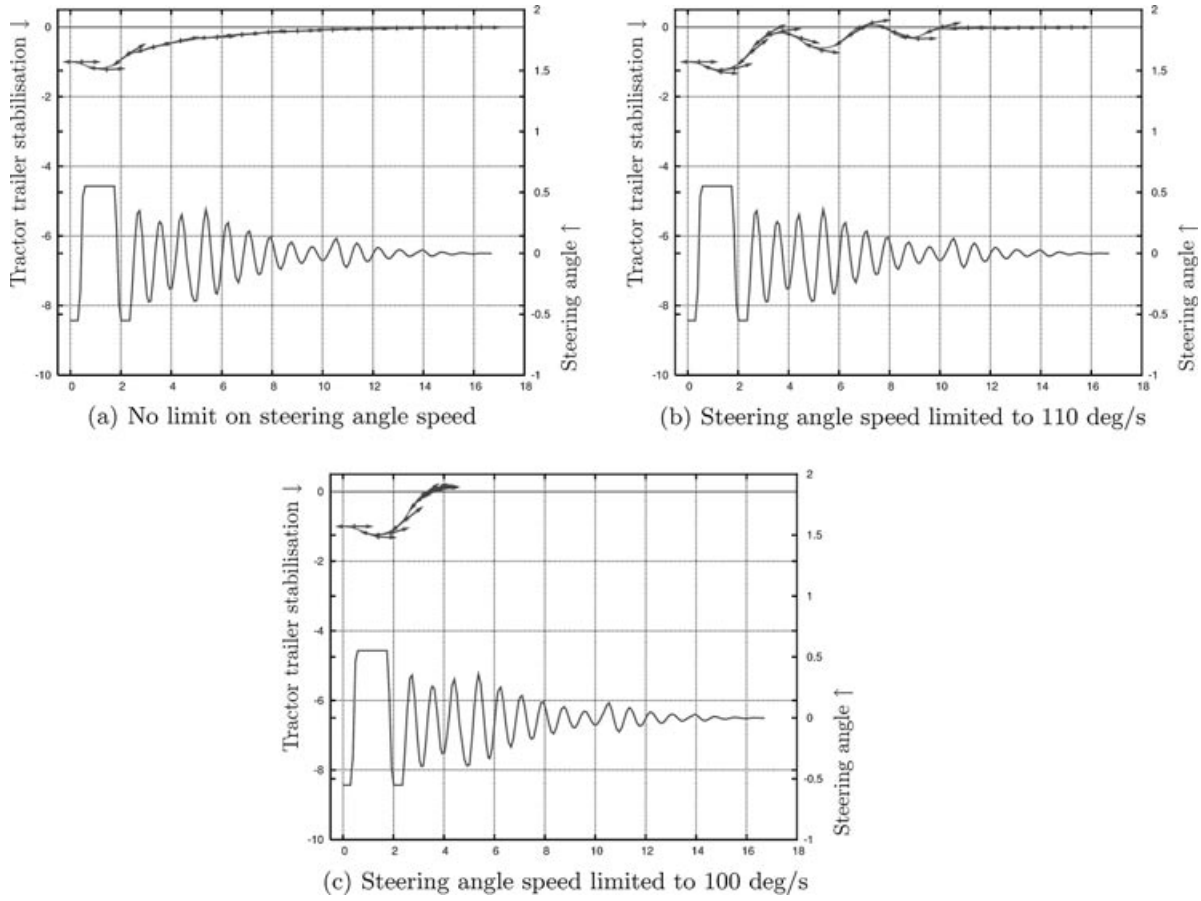

Figure 2. Stabilization of a tractor trailer to a straight trajectory ($y = 0$) using the HILARE controller (Sekhavat et al., 1997), while varying the steering angle rate (simulation). In each graph, the top part of the plot is demand trajectory (straight line) and the path of the vehicle moving from left to right, the arrows showing the heading of the tractor and trailer, and the bottom part shows the steering angle during the maneuver.

3.2. Differential Flatness

In the work of Rouchon, Fliess, Lévine, and Martin (1993), the tractor-trailer system depicted in Figure 1 is classed as a *general one-trailer system*, which has been proved to be differentially flat. Using this property, and inspired by Hermosillo and Sekhavat (2003) and Pradalier et al. (2005), we can convert the trajectory of the tractor-trailer system into the trajectory of its flat output (y_1, y_2):

$$y_1 = x + L_2\cos(\theta+\psi) + L(\psi)\frac{L_2\sin(\theta+\psi) - L_1\sin(\theta)}{\sqrt{L_1^2 + L_2^2 - 2L_1L_2\cos\psi}}, \quad (8)$$

$$y_2 = y + L_2\sin(\theta+\psi) + L(\psi)\frac{L_2\cos(\theta+\psi) - L_1\cos(\theta)}{\sqrt{L_1^2 + L_2^2 - 2L_1L_2\cos\psi}}, \quad (9)$$

with

$$L(\psi) = L_1L_2\int_{\pi}^{2\pi-\psi}\frac{\cos\sigma}{\sqrt{L_1+L_2-2L_1L_2\cos\sigma}}d\sigma.$$

Following Hermosillo and Sekhavat (2003) and Pradalier et al. (2005), a stabilizing control law is

$$y_{i=1,2}^{(3)} = (y_i^\star)^{(3)} + \sum_{j=0}^{2} k_{i,j}\left[y_i^{(j)} - (y_i^\star)^{(j)}\right], \quad (10)$$

where $(y_1^\star, y_2^\star)$ is the flat output corresponding to the state on the reference trajectory and $(.)^{(p)}$ is the time derivative operator of order p.

This technique requires the estimation of the two first derivatives of the state's flat output and then integration of the resulting control in order to deduce the actual steering and speed from the third derivative of the flat output, all of this while using and inverting Eqs. (8) and (9). Even if theoretically stable, the multiple derivatives and integrations make this method extremely sensitive to noise in the state estimation. In a real implementation, the state estimate can be quite noisy, making the second derivative of its flat output close to meaningless.

Our experience (Pradalier et al., 2005) in implementing this type of control law confirms this predicted sensitivity. Moreover, the tuning of the parameters $k_{i,j}$ is difficult due to their sheer number, their coupled effect on all the vehicle states, and the absence of any physical meaning of these parameters.

3.3. Trajectory Stabilization Using Precomputed Gains

Walsh, Tilbury, Sastry, Murray, and Laumond (1994) proposed a control law that, in theory, can exponentially stabilize a tractor-trailer system onto a reference trajectory. In principle, this control scheme estimates a gain for a linear control law on each point of the reference trajectory, using the shape of the trajectory over the next Δt seconds.

In our implementation, this approach presented two main difficulties. First, the precomputation of the gains involves complex integral estimations that can be prohibitively long if the trajectory is longer than a few meters. Second, this method does not provide a way to prioritize the control: When steering a trailer, it is essential to keep the hitch angle stable and controllable because entering a jackknife situation is irrecoverable unless forward motion is instigated. Unfortunately, this method does not provide any mechanism to deal with this constraint.

3.4. Chained-Form Representation

To obtain the chained form for this system, we first use Altafini's (2001) result, which shows that a car-like tractor pulling an off-centered single trailer can be modeled as a standard three-trailer system (that is, one tractor pulling three trailers). From this, the work of Sørdalen (1993) and Tilbury, Sørdalen, Bushnell, and Sostry (1995) gives the transformation of this system into a chained-form representation. The equations for this representation run to several pages in length and are omitted here for brevity.

One of the primary problems with the chained-form representation is that it creates very strong coupling between all the angles of the system; as a consequence, designing a controller and a tuning strategy is as hard as, or even harder than, when using the flatness property of the system.

3.5. Optimal Control

The *optimal control*–based methods use optimization schemes to derive a sequence of demands that will drive the tractor-trailer system onto the desired trajectory or path; see, for example, Altafini, Speranzon, and Wahlberg (2001) and Divelbiss and Wen (1997).

In simple terms, these methods use a vehicle model and a simulation process to compute the control commands that will lead to the best tracking of the trajectory. The required control trajectory can be optimized over some time horizon for minimal time, minimal control effort, or a combination of these and any other relevant "costs."

These methods rely on being able to adequately simulate the vehicle's behavior, which requires considerably more computational resource than would be required for the approach proposed in this paper. Deviations from the model, which in real-world implementations are inevitable, can lead to errors, which requires reestimation of the optimal control sequence. Furthermore, these methods are open loop, meaning that replanning is necessary to deal with errors in localization.

3.6. Learning-Based Approaches

The *learning-based* controllers seek to ease the computational burdens of the previous methods by providing a mapping between the current vehicle state, the desired state, and the required inputs to reach the desired state; see, for example, Koza (1992). Essentially, a simulated model of the tractor-trailer system is used to try many different possible methods and parameters. "Learning" occurs by searching the parameter space for the best set of methods/parameters, which are then encoded into, for example, a neural network or look-up table, which maps the "current" to "desired" configuration.

The main drawback of these techniques is the learning itself: If learning occurs from a model of the system, then errors in the model are clearly problematic; if learning occurs on the real vehicle, then there are safety issues because it is not possible to predict the behavior of the vehicle in the learning phase. Also, even if the best set of parameters performs well in practice, it is hard to guarantee its performance, which can be problematic in an application in which reliability is an issue.

4. OUR APPROACH

Our approach to stabilizing a tractor-trailer system to a trajectory is based on the idea of closing an inner loop around the trailer hitch angle and then treating the vehicle as a "virtual" articulated vehicle for which there are provably stable algorithms for stabilizing to a trajectory (Pradalier & Usher 2007b). We begin the discussion with the outer loop, which stabilizes the vehicle to the trajectory, and then we discuss in more detail the inner, hitch-angle control loop and its stability properties.

4.1. Trajectory Stabilization

To stabilize the vehicle to a trajectory (represented by a sequence of vehicle states indexed by time), we use a path-tracking controller derived for an articulated vehicle and apply an additional controller on the vehicle speed to ensure that the vehicle progresses along the trajectory.

The first important aspect of a tractor-trailer system is that its dynamics are asymmetric. When driving forward, the trailer angle is naturally exponentially stable. When reversing, it is naturally unstable. Consequently we use different control laws for the two situations.

When driving forward, we use a standard trajectory-tracking control law, such as *pure pursuit* (Hebert et al., 1997), and we ignore the trailer. When reversing, we use the trajectory control law presented in Ridley and Corke (2003), where a load haul dump (LHD) vehicle was considered. LHDs are four-wheeled, center-articulated vehicles that are used in underground metalliferous (non-coal) mining operations for the transport of ore.

The control law presented in Ridley and Corke (2003) aims at stabilizing the vehicle on a path, i.e., a two-dimensional curve in the plane. It relies on three error measurements, as depicted in Figure 3: ξ_y, the lateral error; ξ_θ, the heading error; and ξ_κ, the curvature error. The control law is defined as

$$\dot{\psi}^\star = K_y \xi_y + K_\theta \xi_\theta + K_\kappa \xi_\kappa, \tag{11}$$

where K_y, K_θ, and K_κ are tuning parameters.[1] From the hitch-angle derivative, a desired hitch angle $\psi^\star$ is computed by integration.[2] Here, this desired hitch

[1] For operations at higher velocities, these gains are speed dependent (Ridley & Corke, 2003).

[2] In discussions with the implementers of Ridley and Corke (2003) on a real LHD (Duff, Roberts, Corke, Sikka, & Winstanley, 2000; Roberts, Duff, & Corke, 2002), it was found that it may sometimes be necessary to directly set $\psi^\star = K_y \xi_y + K_\theta \xi_\theta + K_\kappa \xi_\kappa$. With this change, the vehicle will tend to straighten instead of bending to correct minor errors as would occur with the integrated version. This can be useful when minor errors are mostly the result of localization noise. In practice, we use the nonintegrated version of the control, and the success of this strategy is borne out in the results.

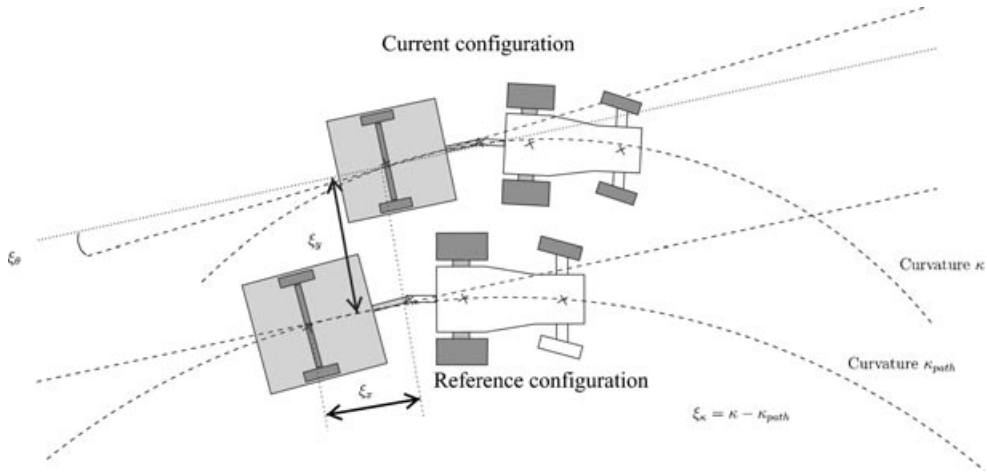

Figure 3. Trajectory error definitions.

angle is then fed into the hitch-angle stabilization law described in the next section. Speed is controlled using a standard pursuit approach to maintain the vehicle's progression along the trajectory and the system switch from the forward control law to the reversing control law when a change of direction is required, as occurs when the onset of jackknifing is detected or there is a cusp in the trajectory [see Pradalier and Usher (2007b) for details]. The trajectory-tracking system is described in block diagram form in Figure 4.

A common problem for such switching controllers is that of "chattering," in which the system gets trapped on the threshold between the two controllers. In this work, we rely on the concept of hysteresis to overcome this problem. For example, on detecting a jackknife situation that requires forward motion for correction, we ensure that the forward motion continues until the hitch-angle error converges to a value 10 times smaller than the jackknife detection value. This is an acceptable behavior because convergence is exponential when driving forward, as shown in Lamiraux (1997).

Of course, more sophisticated switching strategies are available [see, e.g., Campi, Hespanha, and Prandini (2004) and Hespanha, Liberzon, and Morse (2003a, 2003b)], but the hysteresis concept has proven to be sufficient in practice in this instance. However, this strategy assumes that the trajectory has been planned as a smooth path with a relatively low maximum curvature and, consequently, the desired hitch angle $\psi^\star$ is always small. In cases in which this assumption is not valid, it is certainly possible to create situations in which the system will chatter.

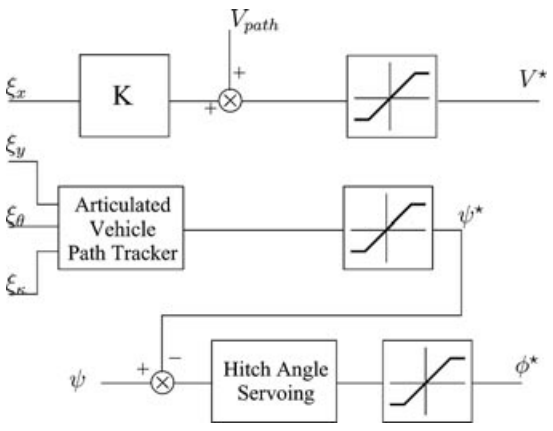

Figure 4. Block diagram for the reversing control law.

4.2. Hitch-Angle Stabilization

We now turn to the critical element in our approach, which is the hitch-angle stabilization loop. The details of this method appear in our previous work on the topic (Pradalier & Usher, 2007a, 2007b), and only an outline is provided here. However, a more detailed formal analysis of the properties of this loop will be presented, from which a nonlinear control

law arises that allows operation over a broader hitch-angle range.

In short, a simple PI controller is enough to achieve the hitch-angle stabilization task:

$$\phi = K_p(\psi^\star - \psi) + K_I \int_0^t (\psi^\star - \psi)du,$$

where $\psi^\star$ is the demanded hitch angle and K_p and K_I are the proportional and integral gains.

Our previous analysis of this controller showed that for nonzero operating points, the control demand needs to be modified in order to compensate for the steady-state error introduced by nonlinearities at these points. Of course, the integral term in the controller would compensate for these effects, but this premodification of the demand speeds up the system response. The expression for modifying the demand such that the system converges to the true demand is

$$\psi^d(\psi^\star) = \frac{K_P L_1 - L + K_P L_2}{K_P(L_1 + L_2)}\psi^\star. \tag{12}$$

Using the above relations, the control law to obtain theoretical convergence on $\psi^\star$ is

$$\phi = K_p[\psi^d(\psi^\star) - \psi] + K_I \int_0^t (\psi^\star - \psi)du. \tag{13}$$

As will be highlighted in the following analysis, the integral term is required to account for minor inaccuracies remaining after the proportional control that can result from the linearization leading to $\psi^d(\psi^\star)$ or from errors in the vehicle model (L, L_1, and L_2).

4.2.1. Stability Analysis

First we assign a Lyapunov function to the system that, in order to prove stability, must be positive semidefinite for all values of the system state. We choose

$$V = \tfrac{1}{2}[\psi^d(\psi^\star) - \psi]^2. \tag{14}$$

The stability of the system can be determined by analyzing $\dot{V} = dV/dt$, i.e.,

$$\dot{V} = \dot{\psi}[\psi - \psi^d(\psi^\star)], \tag{15}$$

where we have used the approximation that $\dot{\psi}^d(\psi^\star) = 0$. This assumption means that we are considering very smooth trajectories, where the rate of variation of the desired trailer angle is small with respect to the variation of the actual angle.

Inserting the control law of Eq. (13) (the proportional component only) and the expression for $\dot{\psi}$ [Eq. (4)] into the above relation leads to

$$\dot{V} = -\frac{v\tan\left\{K_p\left[\psi^d(\psi^\star) - \psi\right]\right\}}{L}\left(\frac{L_1}{L_2}\cos\psi + 1\right) - \frac{v}{L_2}\sin(\psi)$$

after some rearrangement. Figure 5(a) shows a plot of the value of this function across the range of inputs $\psi^\star = [-\pi/2, \pi/2]$ and the output state $\psi = [-\pi/2, \pi/2]$, where $K_P = 1$ has been substituted, and Figure 5(b) highlights the instability points.

These plots indicate that the system is stable for most of the operating region. Exceptions include the "ripples" as indicated in Figure 5(b), but these are avoided in practice by restricting the operating regime. Furthermore, Eq. (16) can be used to monitor the system, altering behavior as appropriate. For example, if Eq. (16) evaluates to a positive number, the reversing maneuver will inevitably lead to a jackknife condition and should be ceased, and a forward correcting motion initiated.

4.2.2. Alternative, Nonlinear Controller

The Lyapunov function analysis from the preceding section can be used to derive an alternative, nonlinear, hitch-angle controller. First we note that the system is stable for $\dot{V} \leq 0$ [where $\dot{V}$ is from Eq. (15)], which can be achieved by setting

$$\dot{\psi} = -K(\psi - \psi^\star), \tag{16}$$

where K is a positive gain. Inserting the expression for $\dot{\psi}$ [Eq. (4)] and rearranging this equation for ϕ leads to the controller

$$\phi = \arctan\left[\frac{L}{v}\frac{K(\psi - \psi^\star) - \frac{v\sin\psi}{L_2}}{\frac{L_1}{L_2}\cos\psi + 1}\right]. \tag{17}$$

This version of the hitch-angle controller theoretically ensures convergence across the range of hitch angle from $-\pi/2$ to $\pi/2$. Additionally, this controller does

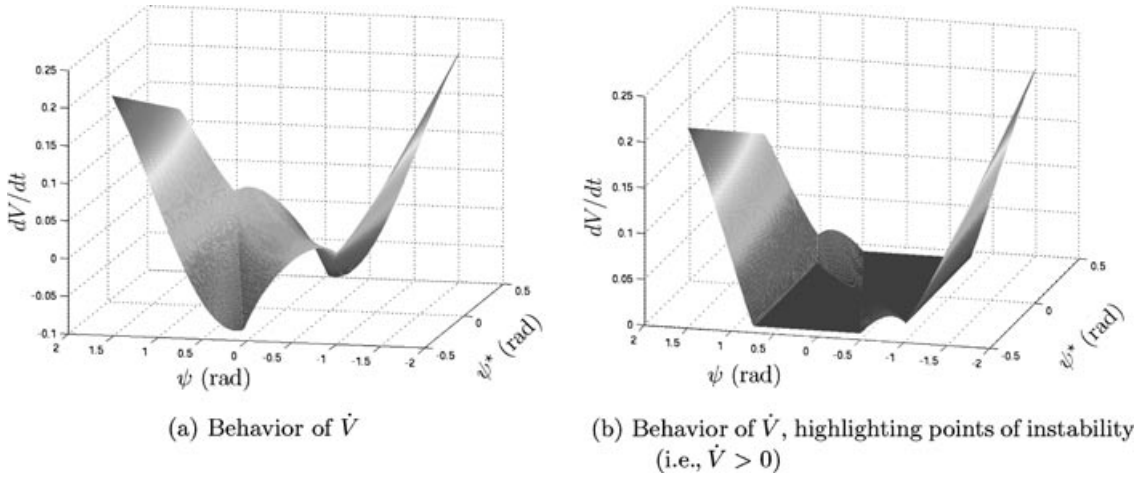

(a) Behavior of $\dot{V}$

(b) Behavior of $\dot{V}$, highlighting points of instability (i.e., $\dot{V} > 0$)

Figure 5. Surface showing the closed-loop behavior of the time derivative of the Lyapunov function $\dot{V}$. Color scale highlights the value of $\dot{V}$.

not require a modification of the demanded hitch angle $\psi^\star$ for nonzero operating points. However, like the controller of Eq. (13), this control law is also sensitive to errors in the system's geometric parameters. Thus, an integral term is required to ensure convergence without steady-state error. In practice, as will be illustrated in Section 6.1., due to the restricted operating range in hitch angle, the performance of this controller is about equivalent to that of Eq. (13).

4.2.3. Can the System Be Linearized?

Analysis of the system is substantially simplified if we can remove its nonlinear elements. To evaluate the linearity of the system, we first look at the closed-loop behavior of the $\dot{\psi}$ dynamics by inserting the control law of Eq. (13) into Eq. (4). Figure 6(a) shows a plot of these dynamics over a feasible range of the state and input space.

If instead we linearize the system about $\phi = 0$ and $\psi = 0$, we have $\tan\phi \approx \phi$, $\cos\psi \approx 1$, and $\sin\psi \approx \psi$, and we obtain the approximated (open-loop) ψ dynamics:

$$\dot{\psi} = -\left[\frac{v}{L}\phi\left(\frac{L_1}{L_2}+1\right) + \frac{v}{L_2}\psi\right], \tag{18}$$

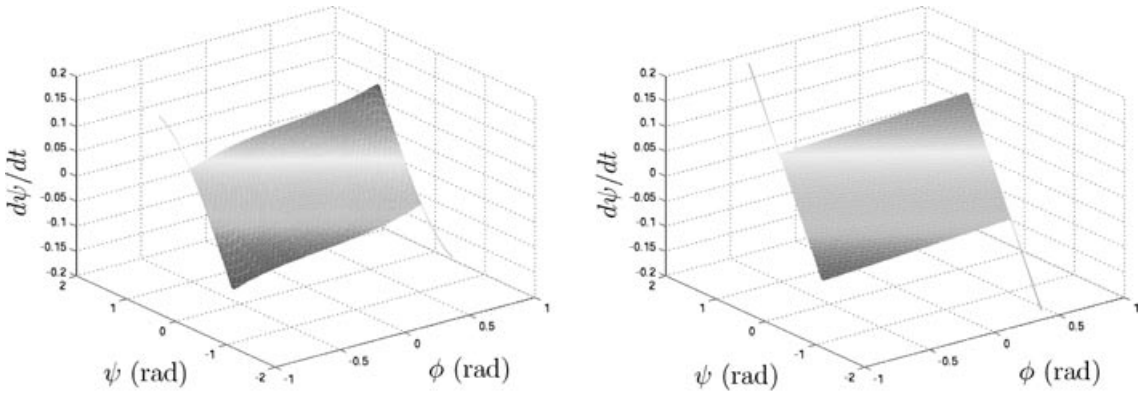

(a) Full nonlinear closed-loop behavior of $\dot{\psi}$

(b) Linearized closed-loop approximation of $\dot{\psi}$

Figure 6. Comparison of full and linearized $\dot{\psi}$ dynamics. Color scale highlights the value of $\dot{\psi}$.

and again inserting the control law of Eq. (13), we obtain the closed-loop behavior for $\dot{\psi}$. Figure 6(a) illustrates the linearized $\dot{\psi}$ dynamics. Comparison with Figure 6(b) shows that the linearized response closely follows the true dynamics for the majority of the workspace and, even at the extremities, exhibits similar behavior.

The ability to linearize the system allows for the use of classical linear control tools for stability analysis and tuning purposes.

4.3. Tuning Strategy

A key advantage of this controller over existing methods is its simplicity, making it easy to implement and tune. The tuning strategy we use consists of three steps:

Tuning of the hitch-angle controller This requires tuning of the parameters K_P and K_I in Eq. (13). A standard proportional integral derivative (PID) tuning technique can be used, based on an analysis of the linearized system. In practice, we first start with $K_P = 1$ and $K_I = 0$, and then initialize the system with a nonzero hitch angle, stabilizing to zero while reversing at constant speed. We then increase K_P until oscillation appears. When K_P is optimal, we increase K_I, and the process is repeated, except in this case it is preferable to stabilize the system to a nonzero hitch angle in order to set the integral gain high enough to account for model errors. This procedure should also give practical bounds on the controllable hitch angles.

Tuning of K_x, K_y, and K_θ These parameters can be tuned by subjecting the system to lateral steps: From a starting position with a null hitch angle, the system must stabilize itself to a straight trajectory with a lateral offset (1 m, for instance), a process illustrated in Figure 7. The initial values of these parameters can be set so as to generate the maximum hitch angle for a given error. For instance, we may want to use the maximum hitch angle when the lateral error $|\xi_y|$ reaches 1.5 m or the heading error $|\xi_\theta|$ reaches 30 deg. During this stage, K_κ should be set to zero.

Tuning of K_κ K_κ has an influence only when driving on curved trajectories. As a consequence, it should be tuned by controlling the system to a circular trajectory with a feasible curvature. Using only K_y and K_θ, the system should be able to closely track a circular path. K_κ adds "look-ahead" by keeping the hitch angle above zero even if the other errors are null. In practice K_κ is less important than the other gains because changing the curvature is, in effect, how we control the trajectory of our system.

4.4. Simulations

Figure 7 shows the resilience of our controller to steering angle rate limitations. From an unlimited steering rate to a maximum of 20 deg/s, the controller was able to correct a 1-m lateral error with a very smooth path. With a maximum steering rate of 15 deg/s, a limit cycle starts to appear but the system still converges. At a rate limit of 10 deg/s, the controller can no longer stabilize the trailer onto the reference path. These results should be compared to those of Figure 2, where the minimum acceptable steering rate was roughly 100 deg/s.

5. EXPERIMENTAL PLATFORM

The platform used in these experiments is the CSIRO Autonomous Tractor (AT), as shown in Figure 8. It is an Ackerman-steered, ride-on mower that has been retrofitted with an array of actuators, sensors, and a computer system enabling the implementation and testing of control and navigation algorithms. The trailer hitch angle is sensed using a set of string pot encoders. Table I summarizes the system geometry with reference to Figure 1. For full details of the vehicle's design, refer to Usher (2005).

5.1. System Dynamics

The dynamics of the underlying control loops are extremely important in the application of trajectory and pose control algorithms to nonholonomic systems. In this section we identify models of the AT's response to steering and velocity inputs, which are subsequently used for system design and analysis purposes.

Table I. Geometric parameters of the CSIRO tractor-trailer system.

Parameter	Value (m)
L	1.2
L_1	0.45
L_2	1.2

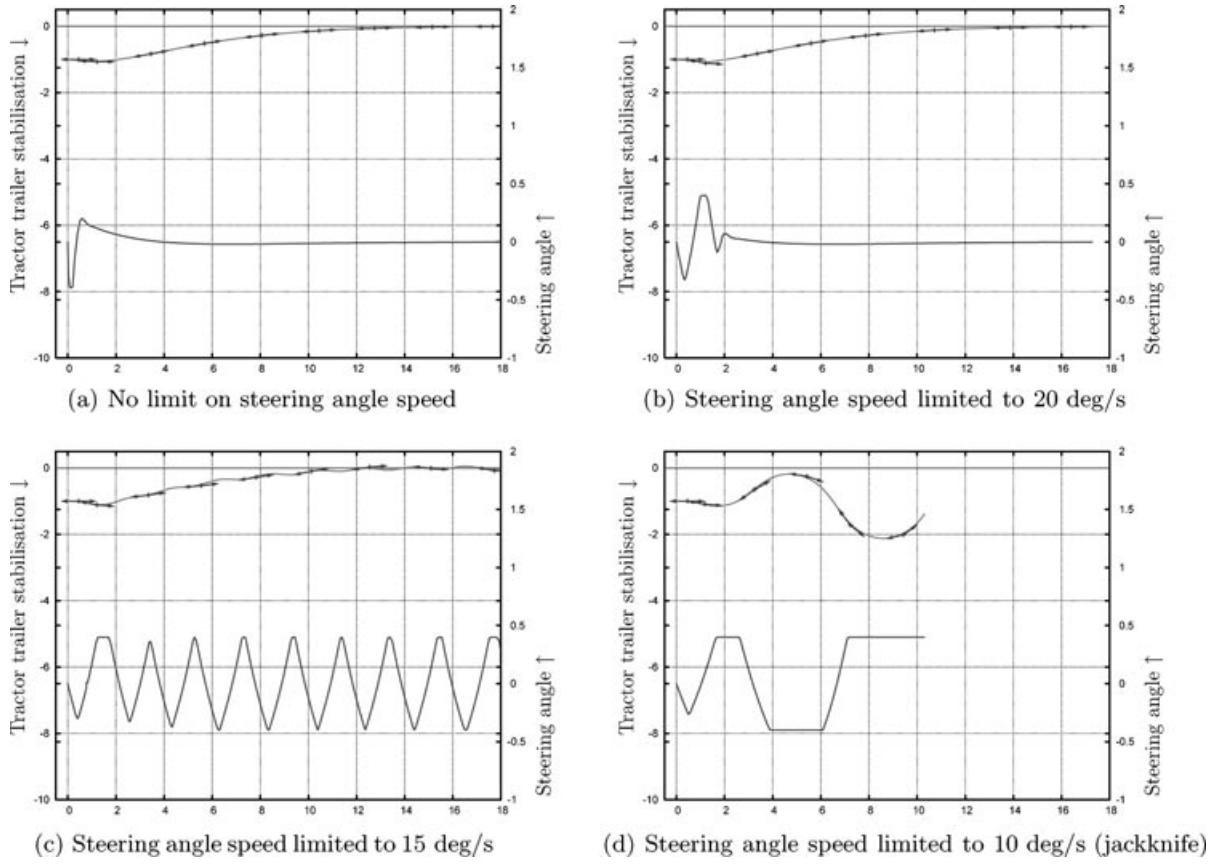

Figure 7. Stabilization of a tractor trailer to a straight trajectory using our approach while varying the steering angle speed (simulation). In each graph, the top part of the plot is the path of the vehicle moving from left to right, arrows showing the heading of the tractor and trailer, and the bottom part shows the steering angle during the maneuver.

5.1.1. Steering

An approximate model of the steering dynamics was experimentally identified from the response of the AT's steering loop to step changes in desired steering angle when traveling in reverse at 0.3 ms^{-1}. The response was determined to be approximately second order of the form (in the Laplace domain)

$$\frac{\phi(s)}{\phi^*(s)} = \frac{\omega_n^2}{s^2 + 2\zeta\omega_n + \omega_n^2}. \tag{19}$$

The parameters ω_n and ζ vary due to the complexity of the interactions between the terrain and the wheels on different surfaces and also with the vehicle's translational speed. For these experiments, parameter values of $\omega_n = 2.15$ and $\zeta = 1.0$ were found to model the system adequately. Additionally, the steering angle range is limited to $\phi_{\max} = \pm 30$ deg and it is rate limited at approximately $\dot{\phi}_{\max} = \pm 20$ deg/s. Figure 9(a) shows a plot of the actual and modeled response of the vehicle to a step input.

5.1.2. Velocity

The velocity loop was empirically determined to have a first-order response, which is represented in the Laplace domain as

$$\frac{v(s)}{v^*(s)} = \frac{K_v}{\tau_v s + 1}. \tag{20}$$

Figure 9(b) illustrates the AT's response to a unit step change in velocity while traveling on level ground (concrete) and the response of the first-order model where $K_v = 1$ and $\tau_v = 1.33$. Again, the model

Figure 8. The AT with its trailer.

parameters will vary on sloping terrain, on different surfaces, and under different loading conditions. In addition, the speed of the AT is constrained to the range $-1.5\ \text{ms}^{-1} < v < 3\ \text{ms}^{-1}$.

In practice, the velocity loop has little impact on the overall system dynamics, and thus the primary focus in this work is on the analysis of the system, including the steering-loop dynamics.

5.2. Hitch-Angle Control System Modeling

We now consider a linear model of the hitch-angle control loop for the AT. In this analysis, we consider the controller of Eq. (13) and, to ease the analysis, ignore the effects of the integral term in the controller.

The steering loop dynamics are modeled by Eq. (19), and the linearized hitch-angle dynamics are represented (after the introduction of an intermediary state for the steering) by

$$\begin{bmatrix} \dot{\rho} \\ \dot{\phi} \\ \dot{\psi} \end{bmatrix} = \begin{bmatrix} 0 & -\omega_n^2 & \omega_n^2 K_P \\ 1 & -2\zeta\omega_n & 0 \\ 0 & -\frac{v}{L}\left(\frac{L_1}{L_2}+1\right) & -\frac{v}{L_2} \end{bmatrix} \begin{bmatrix} \rho \\ \phi \\ \psi \end{bmatrix} + \begin{bmatrix} \omega_n^2 K_P \frac{(L_1+L_2)+L}{(L_1+L_2)} \\ 0 \\ 0 \end{bmatrix} \psi^*, \tag{21}$$

$$\dot{x} = A \cdot x + B \cdot u. \tag{22}$$

5.2.1. Root Locus

The characteristic equation for this system can be found by calculating the determinant of $sI - A$, where A is the state transition matrix. The characteristic equation for this system is

$$s^3 + \left(\frac{v}{L_2} + 2\zeta\omega_n\right)s^2 + \left(\frac{2\zeta\omega_n v}{L_2} + \omega_n^2\right)s - \omega_n^2 \frac{v}{L_2}\left[1 - \frac{K}{L}(L_1 + L_2)\right]. \tag{23}$$

By placing Eq. (23) in the form $1 + K_P GH = 0$, we can observe the behavior of the roots of the characteristic equation for various values of K_P. The resulting root locus plot is shown in Figure 10. The root locus indicates that the system is stable for $0.72 < K_P < 9.68$, and for a critically damped system, the gain should be set to $K_P = 1.65$.

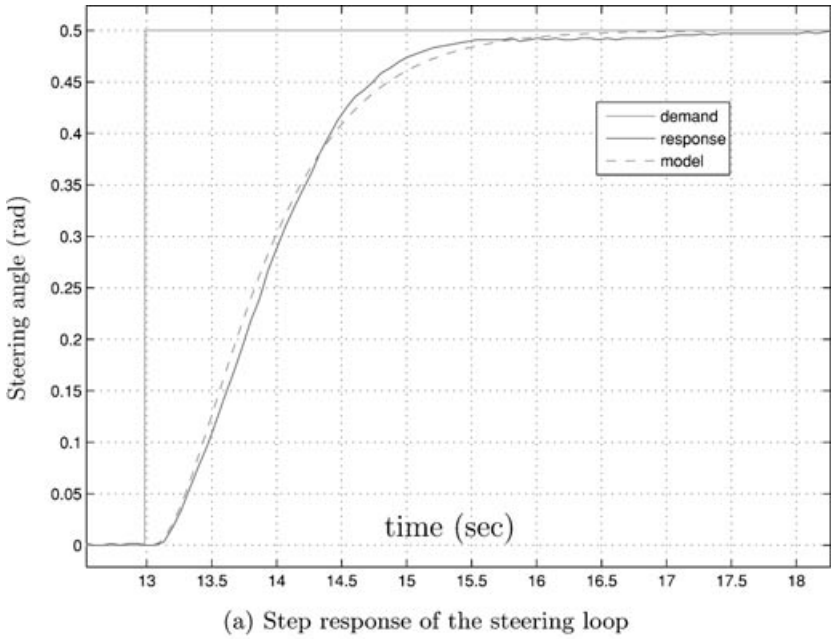

(a) Step response of the steering loop

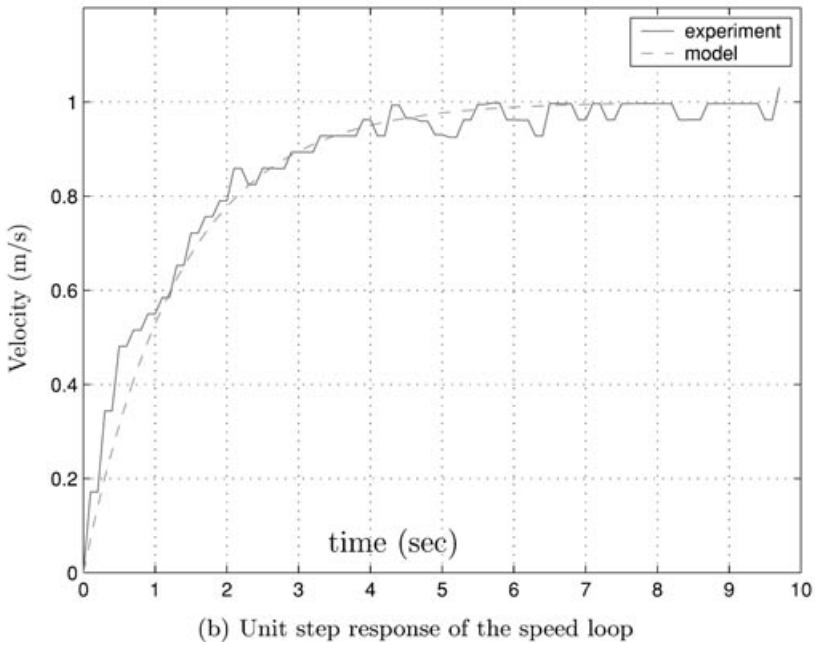

(b) Unit step response of the speed loop

Figure 9. Step response of the steering and velocity loops. Model data are plotted as a dashed line and experimental data as a solid line.

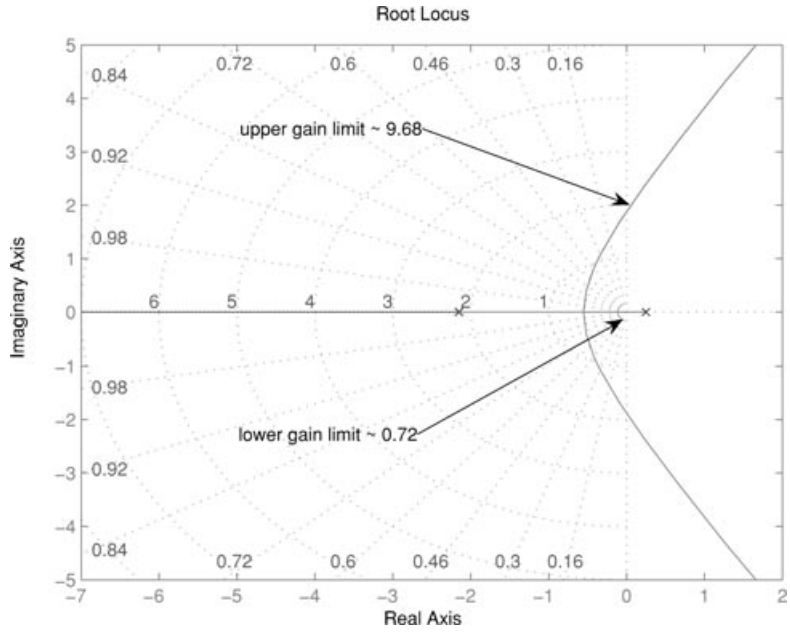

Figure 10. Root locus plot for the closed-loop system, including the steering loop dynamics, using the linear P controller.

5.2.2. Sensitivity Analysis

We now turn to an analysis of the sensitivity of the system to parameter variations. First, we present the case for the parameter L, following which a summary of the results for the remaining parameters is presented.

To determine the system's sensitivity to L, we evaluate

$$S_{s.L} = \frac{L}{s}\frac{\partial s}{\partial L}, \tag{24}$$

which results in

$$\frac{\frac{\omega_n^2 K_P v(L_1+L_2)}{LL_2}}{3s^3 + \left(\frac{2v}{L_2} + 4\zeta\omega_n\right)s^2 + \left(\omega_n^2 + \frac{2\zeta\omega_n v}{L_2}\right)s}.$$

We now evaluate this sensitivity at two representative levels of system gain K_P, using the root locus of Figure 10 to determine the dominant poles at these points:

$$K_P = 1.23: \quad s = -0.357, \qquad S_{s.L} = -5.27,$$
$$K_P = 3.10: \quad s = -0.362 \pm 1.0i, \; S_{s.L} = 0.40 \angle 141\text{deg}.$$

This indicates that the poles in the system are very sensitive to changes in the parameter L and that this sensitivity is substantially reduced with increasing gain.

We can also evaluate the effect of a change in L on the position of the dominant pole by rearranging Eq. (24):

$$\Delta s = s S_{s.L}\frac{\Delta L}{L}.$$

At the gain $K_P = 1.23$ (where the mathematics are more straightforward), a 10% increase in L yields $\Delta s = 0.19$, or a shift to the right of 0.19 units for a 10% increase in L.

Table II summarizes the results of this analysis for the two selected gains analyzed above. With the exception of L_2, which appears to bear little influence over the system sensitivity, the system is similarly sensitive to the other parameters at the lower gain, with a vastly reduced sensitivity at the higher gain. Practically, this analysis implies that the system parameters should be measured with reasonable accuracy and that some form of integral action is required in the controller to accommodate any errors in these measurements.

Table II. System sensitivity to variations in geometric parameters and vehicle velocity.

	$\|\|S_{s.P}\|\|$	
Parameter (P)	$K_P = 1.23$	$K_P = 3.10$
L	5.270	0.390
L_1	47.600	0.018
L_2	0.015	0.001
v	125.790	0.110

5.2.3. Gain Tuning

In practice, the system was tuned using the methods of Section 4.3. For the hitch-angle stabilization loop, gains of $K_P = 4$, $K_I = 0.03$ were found to provide both quick and accurate response with minimal overshoot, whereas for the trajectory-tracking loop, gains of $K_x = 2$, $K_y = 0.2$, $K_\theta = 1$, and $K_\kappa = 0.05$ were found to give the desired behavior.

6. RESULTS

This section presents results obtained when tracking various reversing trajectories, first controlling only the hitch angle, then controlling the tractor's position using odometry-based localization, and then conducting several tests using an external localization estimate. The external localization estimates are provided by a particle-filter–based method using the vehicle odometry and sparse reflective beacons sensed with a front-mounted laser range finder [details on the localization system can be found in Duff, Usher, and Ridley (2006)]. This localization estimate is "drift-free" but comes at the cost of localization discontinuities when corrections are applied on spotting a beacon. Such discontinuities are especially challenging for the trajectory-tracking system.

6.1. Hitch-Angle Controller

Figure 11 shows experimental tests comparing the linear [Eq. (13)] and nonlinear [Eq. (17)] hitch-angle controllers, in which the tractor was reversing at a constant speed of 0.3 m/s. From these plots, we note that the linear and nonlinear controllers give very similar performance in terms of accuracy of the tracking and control of the oscillations. The oscillations of the hitch angle around the nominal trajectory are caused by slop in the hitch-angle sensing and a limit cycle caused by the steering rate limit. On the basis of these results, and for the sake of controller simplicity, we chose to use the linear controller for the following experiments.

6.2. Reversing on a Circle with Fixed Radius

In the first set of experiments, we define reference trajectories as arcs of circles of various radii. The pose of

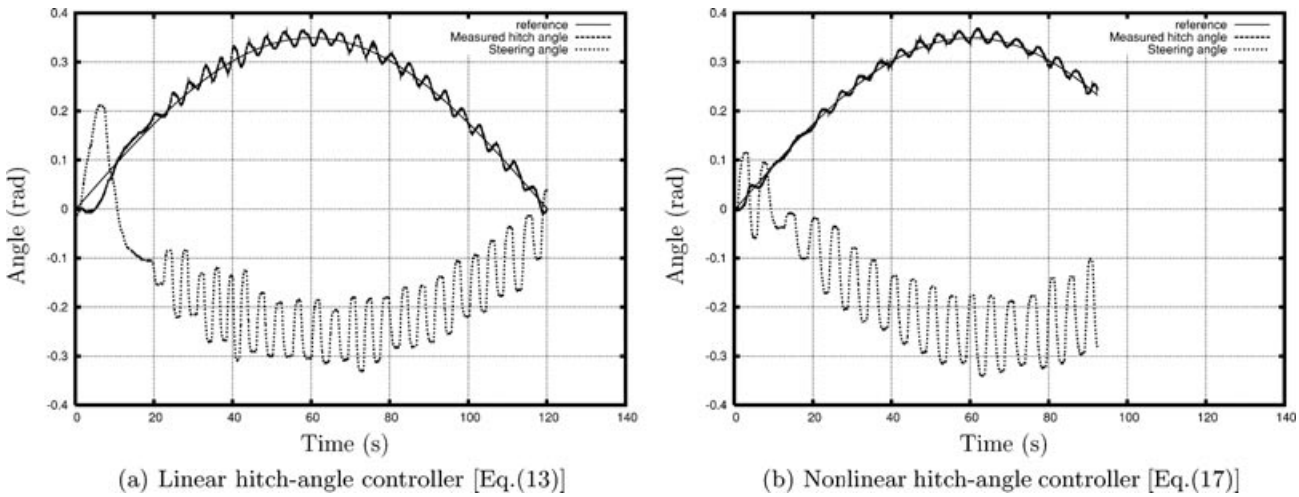

(a) Linear hitch-angle controller [Eq.(13)] (b) Nonlinear hitch-angle controller [Eq.(17)]

Figure 11. Experimental performance comparison of the linear and nonlinear hitch-angle controllers in following a sinusoidal input. Reference trajectory is shown as a solid line, actual trajectory as a dashed line, and steering angle input as a dotted line.

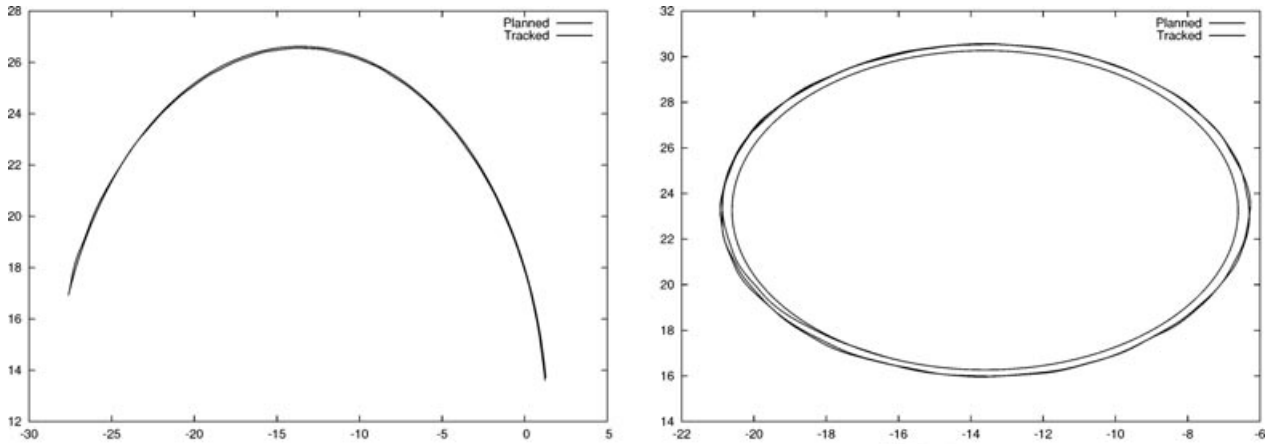

Figure 12. Trajectory tracking with odometry-based localization.

the vehicle is computed using odometry information. The advantage of this setting is that the vehicle pose is a very clean and smooth signal. The disadvantage is that odometry localization is known to drift over time and, consequently, is not suitable for real-life, long-range, robotic operations.

Figure 12 shows tracking results for a circular path, with radii of 7.5 and 15 m. As can be observed, the tracking is very accurate for radii of 15 m. For a radius of 7.5 m, the maximum achievable curvature is reached and the system cannot converge to the required trajectory. However, it should be noted that the system converges to a stable orbit, which is the best it can do to follow the required curvature.

6.3. Reversing on a Badly Planned Trajectory

In the second set of experiments, we stretch the system by introducing a more complex path, as depicted in Figure 13(a). We consider this trajectory to be "badly planned" because it does not take into account the limitations of the vehicle, especially the limited turning radius and the very strong limitation on the hitch-angle rate. In addition, the trajectory contains path discontinuities in which straight lines join circular segments; such discontinuities are challenging for the control law because they require a very fast change of hitch angle. Our objective here is to show the performance of our system at the limits of its nominal specification. To further challenge the controller, we also use the external localization system rather than the vehicle odometry.

Figure 13(b) illustrates how the planned path is tracked by our tractor-trailer systems. From this experiment, we note that on straight-line segments the system converges reasonably fast. On the curved segments, the curvature is beyond the vehicle capabilities and the tracked trajectory is offset from the planned one. Transitions between the curved and straight segments of the path (Events 5, 8, and 9) introduce a discontinuity that the system struggles to deal with but nevertheless recovers from. Localization discontinuities (Events 6 and 7) are handled much more gracefully than the path discontinuities. Finally, Event 5 is an occurrence of a situation in which a beginning of jackknife was detected and the vehicle had to drive forward for approximately 2 m to restabilize the trailer, before continuing reversing.

From these experiments, it is clear that in order to obtain very accurate tracking, the path planner needs to take into account the strong constraints of this system, in particular, the small maximum trackable curvature and the need for smooth curvature profiles. However, the trajectory control performed extremely well within these constraints.

6.4. Reversing on a Preplanned Trajectory

In this set of experiments, our objective was to demonstrate the performance of our system in a real-world situation. To this end, we designed a path across our research center. This path is approximately 170 m long and was planned manually using hand-selected way points and interpolating splines. This

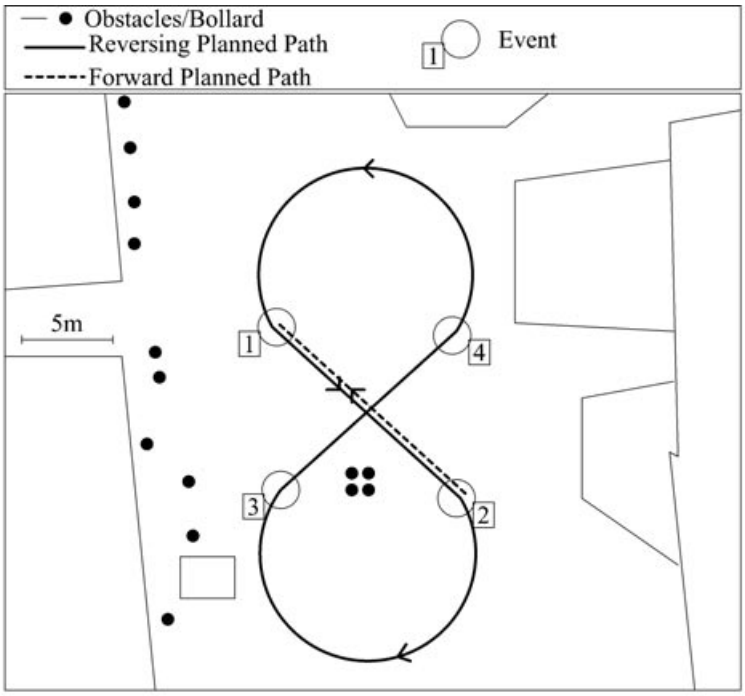

(a) Schematic of the planned trajectory

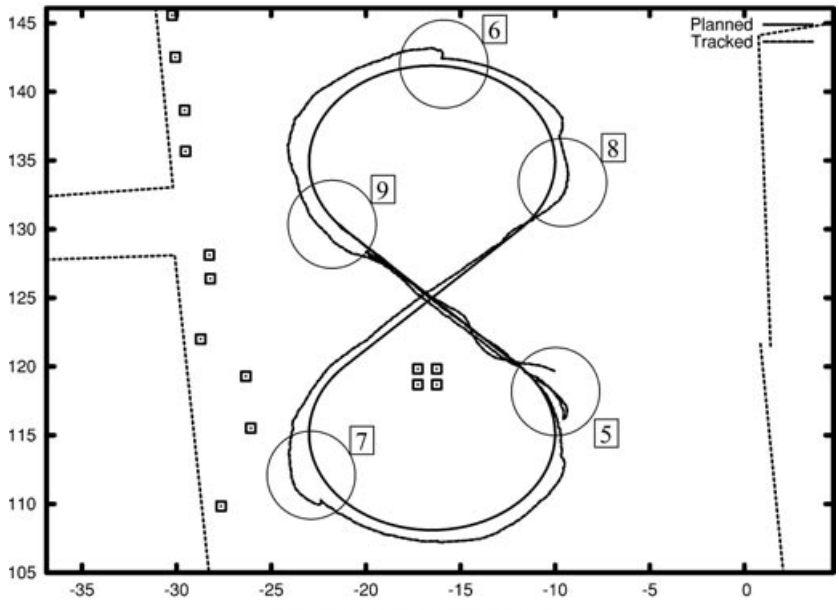

(b) The tracked trajectory

Figure 13. Performance for a poorly planned trajectory that does not account for curvature limitations or path discontinuities. *Events* are denoted by the boxed numbers.

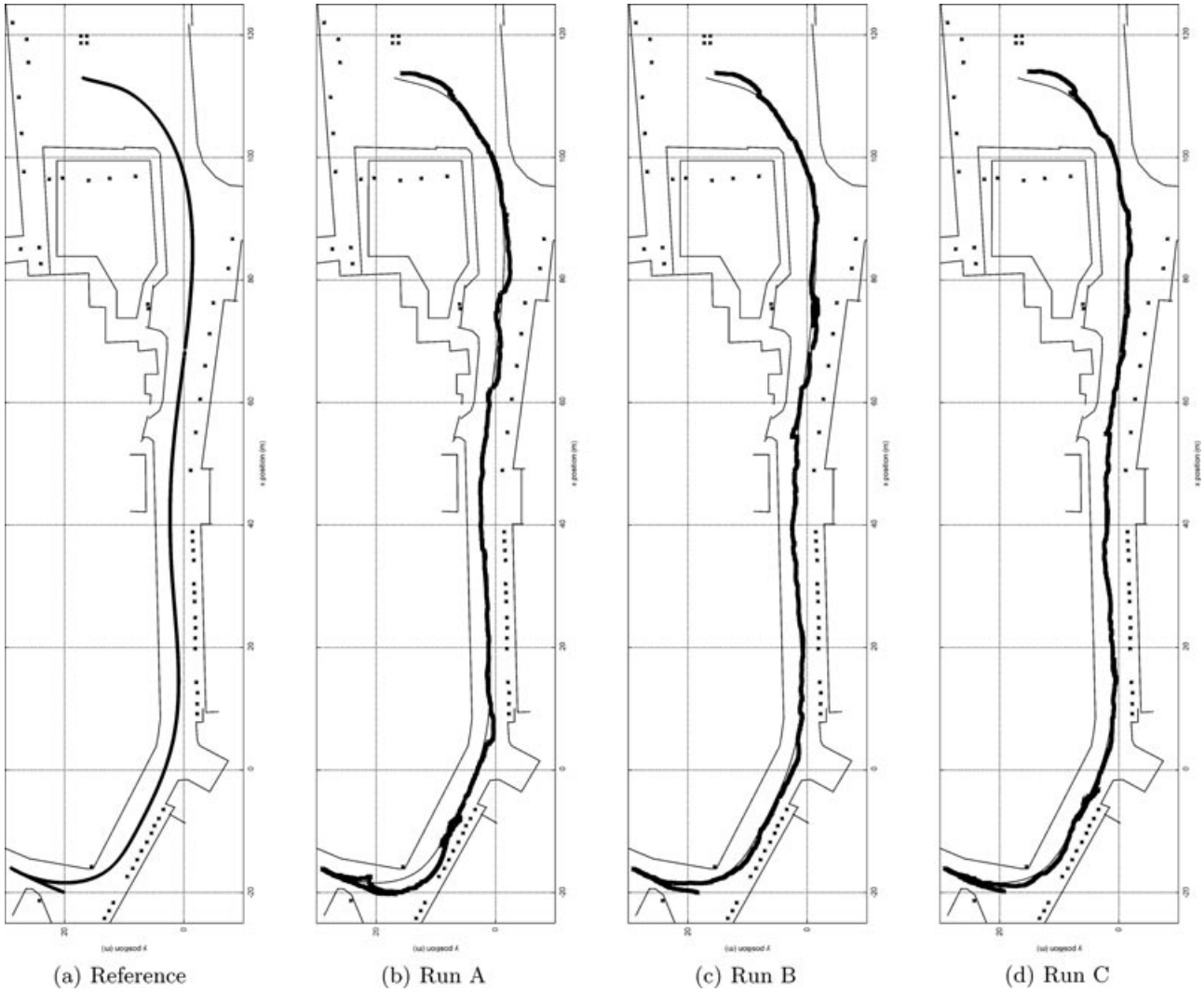

Figure 14. Reversing trajectories of the autonomous system on three independent runs.

approach guarantees a smooth and continuous trajectory. For these experiments, the system relied on the external localization estimates.

The resulting path is depicted in Figure 14(a). It is composed of two segments: a short forward motion to help align the system with the trajectory and a long reversing segment of approximately 160 m. The main constraints when designing this trajectory were to keep the vehicle close to the middle of the road and to minimize the path curvature.

Figures 14(b)–14(d) show the trajectories realized by our controller on three separate runs. More accurately, the trajectories represent the path of the center of the AT's rear axle. Examples of localization jumps (corrections) can be seen at the top end of all trajectories and around $(55, 0)$ in Runs B and C. It is important to note that our system stays stable around the reference trajectory, even when the localization estimation is very unstable. In some situations, e.g., close to $(-10, 10)$ in Runs A and C, or close to $(75, 0)$ in Run B, the localization estimate oscillates between the two sides of the reference trajectory. If this occurs at the wrong frequency, it can bring the system to a jackknife situation. In all cases, the preliminary signs of

Table III. Summary of experimental run statistics, for human and autonomous drivers.

Subject	Graph Label	Experience	Duration (s)	Corrective Fwd Motions	Avg Speed (m/s)
1	1	Professional	160	0	1.12
2	2	Beginner	300	4	0.60
3, Run 1	3	Beginner	322	3	0.55
3, Run 2	4	Beginner	230	2	0.78
4, Run 1	5	Medium	278	2	0.64
4, Run 2	6	Medium	290	2	0.62
5, Run 1	7	Medium	400	2	0.45
5, Run 2	8	Medium	250	0	0.72
6	9	First time	980	14+	0.18
Auto A	10	Autonomous	620	1	0.29
Auto B	11	Autonomous	600	1	0.3
Auto C	12	Autonomous	628	2	0.29

this event were detected by the system, and a short forward motion was initiated to realign the vehicle with the reference trajectory.

6.5. Evaluation: Comparison with Human Drivers

As a final experimental evaluation of our reversing system, we tested a number of human drivers in performing a trajectory similar to that performed by the autonomous system outlined in Section 6.4. Skill levels of these drivers were the following:

First time: first experience of trailer reversing
Beginner: driver having reversed a trailer a couple of times in recreational activities
Medium: driver who regularly reverses trailers in recreational activities
Professional: professional truck driver

For practical reasons, the drivers were required to keep the vehicle in the middle of the road, rather than following the same trajectory as the automated system.

We evaluated the drivers' ability to stabilize the trailer and to avoid jackknife situations and the statistical properties of their steering input. Figure 15 shows an example of human-controlled trajectories, in comparison with autonomous system ones.

6.5.1. Trajectories

These experiments were conducted using six drivers, some of whom drove the trajectory twice. Some statistics about the drivers' performances are presented in Table III. Examples of trajectories realized by representative subjects are presented in Figure 14(d), where the paths were recorded using the external localization system.

When comparing the performance of human drivers with the autonomous control, one obvious difference is the travel speed. Except for the driver who was reversing a trailer for the first time, all human drivers were much faster than our system. As we will see later, this is mainly a result of the limited actuation capabilities of the autonomous system; to compensate for these limitations, the system has to be artificially slowed down.

Concerning the trajectories, the autonomous system realizes smoother paths than the inexperienced drivers and drives in a similar fashion as the more experienced human drivers. This is a definitive achievement given the limited actuation and the fact that the control relies on localization estimates, which can be discontinuous.

6.5.2. Hitch-Angle Stabilization

Figure 16(a) depicts the statistical properties of the measured hitch angle for each run as box diagrams. Each box represents the statistical distribution of measured hitch angles through its five-number summaries [the smallest observation, lower quartile (Q1), median, upper quartile (Q3), and largest observation]. If we call IQR the interquartile range, i.e., Q3 − Q1, then any data more than 1.5 IQR from the closest quartile (Q1 or Q3) are considered outliers. Graphically, the boxes in this diagram show the Q1 − Q3 interval: The "whiskers" show the farthest data

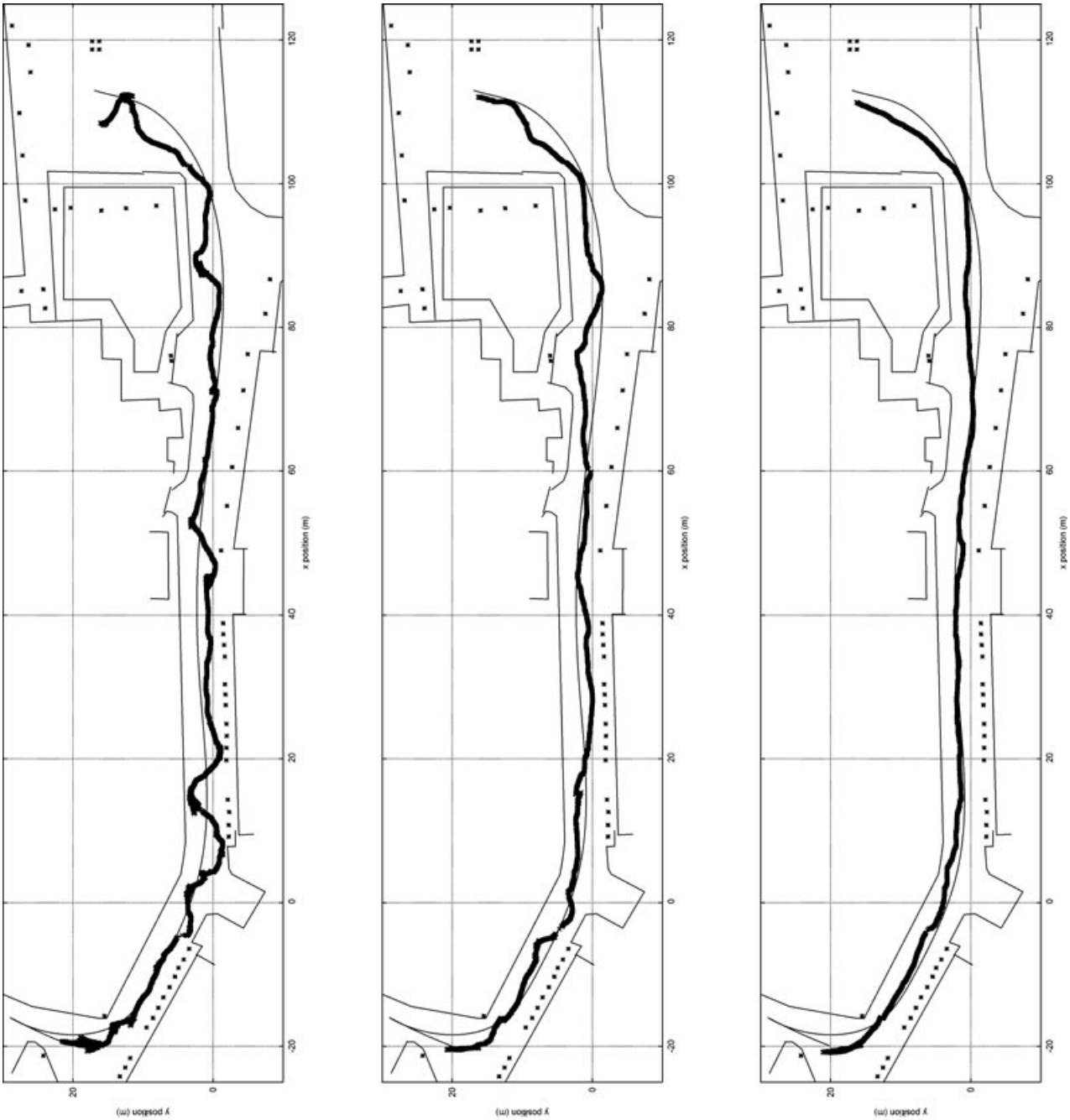

(a) Subject 6 (first time)

(b) Subject 4, Run 1 (medium skill)

(c) Subject 4, Run 2 (medium skill)

Figure 15. Reversing trajectories of inexperienced to medium drivers. Numbers correspond to those in Table III.

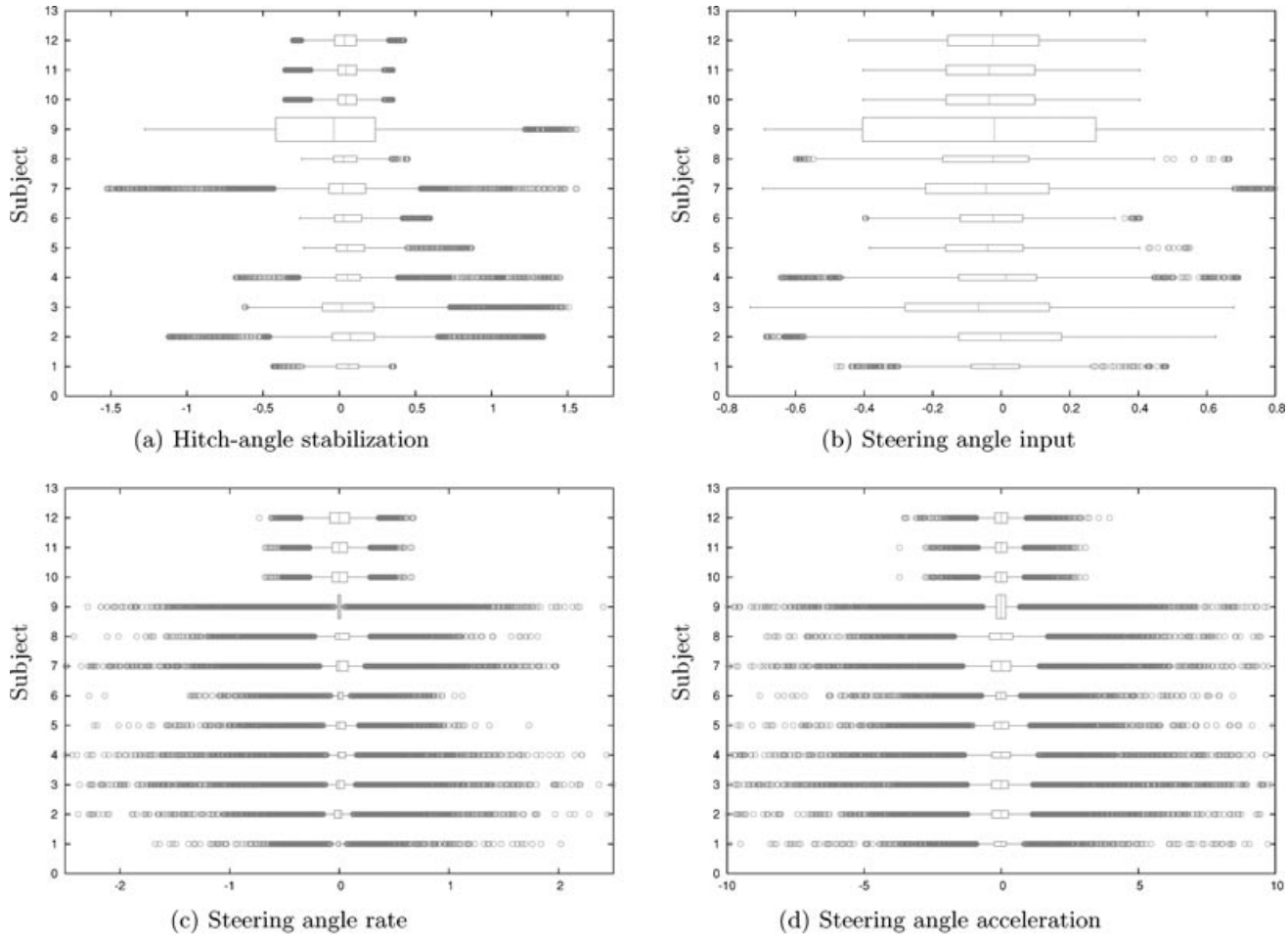

Figure 16. Comparisons of the capabilities of human drivers and the autonomous system. Numbers correspond to those given in the Graph label column of Table III. Lines 10–12 correspond to the three runs of the autonomous system.

point from the quartiles that is not considered an outlier, and the red circles show points considered outliers. The height of the boxes is not meaningful in our analysis.

In practice each line represents one run, with numbers referring to the different subjects in Table III. Lines 10–12 refer to the autonomous runs. The width of a box with its whiskers gives the range of steering angle regularly used by the driver. The red circles depict the steering angle used by the driver in infrequent events, such as the correction of the beginning of a jackknife situation. Jointly, the boxes and the circles give the range of control the driver (human or autonomous) used to achieve the trajectory.

For the autonomous runs, we note that the median hitch angle is slightly shifted toward positive values. This is expected because the trajectory is close to a long right-hand turn. When comparing the hitch-angle range of the autonomous system with that of the human drivers, it is clear that the autonomous system keeps much tighter control of the angle than most of the human drivers and is comparable with the professional driver (Driver 1). Nevertheless, it must be noted that this performance is achieved at the cost of a much lower ground speed (0.3 instead of 1.0 m/s).

Figures 16(b)–16(d) illustrate the properties of the steering angle and its first derivative, recorded for the

human drivers and the autonomous system. These graphs demonstrate the reduced control range and capabilities available to the autonomous system in comparison with the capabilities of human drivers: The accessible steering range available to the automation system is reduced by 40% in comparison to the human drivers, and the accessible steering speed and steering acceleration are reduced by about 70%. From these observations, it is clear that human drivers use their additional range of control to drive faster while demonstrating similar hitch-angle stabilization performance.

Finally, it is interesting to note that with driving capabilities reduced by 70%, the performance of our system is similar to that of a professional driver, albeit with a velocity reduced by about 70%. We are yet to determine whether this is a coincidence.

7. CONCLUSION

This article evaluated a new control scheme for a tractor-trailer system. This scheme is based on a two-layer control loop: First a hitch-angle stabilization loop controls the angle between tractor and trailer, and then a path-tracking control loop, initially designed for an articulated mining vehicle, is adapted to our tractor-trailer system.

The main advantage of this approach over traditional methods is its simplicity of implementation. Only a few parameters need to be tuned, and they all have a clear physical meaning. Although simple, this control scheme relies on a mathematically sound background.

Finally, this control law was implemented on a real vehicle and experiments were conducted on challenging trajectories. Given the limited dynamic performance of our platform (slow response time, loose components, low speed actuation), the control law exhibited excellent convergence and stability properties. Furthermore, our controller also compared well with a range of human drivers on a similar trajectory, even though the control system is significantly handicapped in terms of its actuation capabilities.

ACKNOWLEDGMENTS

This work was funded by the CSIRO ICT Centre under the ROVER and Dependable Field Robotics projects. The authors thank the Autonomous Systems Laboratory team for their support of this work. Special thanks go to Polly Alexander, Stephen Brosnan, Peter Corke, Elliot Duff, Paul Flick, Leslie Overs, Ashley Tews, John Whitham, and Graeme Winstanley, who all contributed to the development of our experimental autonomous tractor.

REFERENCES

Altafini, C. (2001). Some properties of the general n-trailer. International Journal of Control, 74(4), 409–424.

Altafini, C., Speranzon, A., & Wahlberg, B. (2001). A feedback control scheme for reversing a truck and trailer vehicle. IEEE Transactions on Robotics and Automation, 17(6), 915–922.

Campi, M. C., Hespanha, J. P., & Prandini, M. (2004). Cautious hierarchical switching control of stochastic linear systems. International Journal of Adaptive Control and Signal Processing, 18, 319–333.

Carter, D., & Lormor, J. (2004). Vehicle steering aid system. GB patent GB2398050.

De Luca, A., & Oriolo, G. (1995). Modelling and control of nonholonomic mechanical systems. In Kinematics and Dynamics of Multi-Body Systems. CISM Courses and Lectures, vol. 360, pp. 277–342. Vienna: Springer-Verlag.

Divelbiss, A., & Wen, J. (1997). Trajectory tracking control of a car-trailer system. IEEE Transactions on Control Systems Technology, 5(3), 269–278.

Duff, E., Roberts, J., Corke, P., Sikka, P., & Winstanley, G. (2000). Autonomous underground mining vehicle final report (Internal Tech. Rep. CMST-BCC2000-22). Brisbane, Australia: CSIRO.

Duff, E., Usher, K., & Ridley, P. (2006). Swing loader traffic control (Tech. Rep. ICT 06/142). Brisbane, Australia: CSIRO ICT Centre.

Hebert, M., Thorpe, C., & Stentz, A. (1997). Intelligent unmanned ground vehicles: Autonomous navigation research at Carnegie Mellon. New York: Kluwer Academic Publishers.

Hermosillo, J., & Sekhavat, S. (2003). Feedback control of a bi-steerable car using flatness: Application to trajectory tracking (volume 4, pp. 3567–3572). In Proceedings of the American Control Conference. New York: IEEE.

Hespanha, J. P., Liberzon, D., & Morse, A. S. (2003a). Hysteresis-based switching algorithms for supervisory control of uncertain systems. Automatica, 39, 263–272.

Hespanha, J. P., Liberzon, D., & Morse, A. S. (2003b). Overcoming the limitations of adaptive control by means of logic-based switching. Systems & Control Letters, 49, 49–65.

Karl, S. (1987). Automatic reverse steering system for passenger vehicles with trailer. DE patent DE3538338.

Koza, J. (1992). A genetic approach to finding a controller to back up a tractor-trailer truck (pp. 2307–2311). In Proceedings of the 1992 American Control Conference. IEEE.

Lamiraux, F. (1997). Robots mobiles remorque: de la planification de chemins l'execution de mouvements. Ph.D. thesis, Polytechnic National Institute of Toulouse, France.

Pradalier, C., Hermosillo, J., Koike, C., Braillon, C., Bessière, P., & Laugier, C. (2005). The cycab: A car-like robot

navigating autonomously and safely among pedestrians. Robotics and Autonomous Systems, 50(1), 51–68.

Pradalier, C., & Usher, K. (2007a). Experiments in autonomous reversing of a tractor trailer system. In Proceedings of the International Conference on Field and Service Robotics, Chamonix, France. New York: Springer-Verlag.

Pradalier, C., & Usher, K. (2007b). A simple and efficient control scheme to reverse a tractor-trailer system on a trajectory (pp. 2208–2214). In Proceedings of IEEE International Conference on Robotics and Automation, Rome, Italy. IEEE.

Ridley, P., & Corke, P. (2003). Load haul dump vehicle kinematics and control. Journal of Dynanic Systems, Measurement and Control, 125, 54–59.

Robert, S. (2004). Trailer backing up device and method. U.S. patent US2004215374.

Roberts, J., Duff, E., & Corke, P. (2002). Reactive navigation and opportunistic localization for autonomous underground mining vehicles. International Journal of Information Sciences, 20, 127–146.

Rouchon, P., Fliess, M., Lévine, J., & Martin, P. (1993). Flatness and motion planning: The car with n-trailers (pp. 1518–1522). In Proceedings of European Control Conference, Groningen.

Sekhavat, S., Lamiraux, F., Laumond, J., Bauzil, G., & Ferrand, A. (1997). Motion planning and control for hilare pulling a trailer: Experimental issues (volume 4, pp. 3306–3311). In Proceedings of IEEE International Conference on Robotics and Automation. New York: IEEE.

Sørdalen, O. (1993). Conversion of the kinematics of a car with *n* trailers into chained form (pp. 802–819). In Proceedings of the IEEE International Conference on Robotics and Automation. New York: IEEE.

Tilbury, D., Sørdalen, O., Bushnell, L., & Sastry, S. (1995). A multisteering trailer system: Conversion into chained form using dynamic feedback. IEEE Transactions on Robotics and Automation, 11(6), 807–818.

Usher, K. (2005). Visual homing for a car-like vehicle. Ph.D. thesis, Queensland University of Technology, Brisbane, Australia.

Walsh, G., Tilbury, D., Sastry, S., Murray, R., & Laumond, J. (1994). Stabilization of trajectories for systems with nonholonomic constraints. IEEE Transactions on Robotic and Automation, 39(1), 216–222.